Programmable long period grating in a liquid core optical fiber

Tao Qi[1,*], Yongmin Jung[2,*], Limin Xiao[3], Jie Wang[4], Shilin Xiao[1], Chao Lu[4], Hwa-yaw Tam[4], and Anna C. Peacock[2]

[1] *The State Key Laboratory of Advanced Optical Communication Systems and Networks, Shanghai Jiao Tong University, Shanghai 200240, China*
[2] *Optoelectronics Research Centre, University of Southampton, Southampton SO17 1BJ, UK*
[3] *Key Laboratory for Micro and Nano Photonic Structure, Department of Optical Science and Engineering, Fudan University, Shanghai 200433, China*
[4] *Photonics Research Center, The Hong Kong Polytechnic University, Hong Kong SAR, China*
[*] *Corresponding author: qtwhat@gmail.com, ymj@orc.soton.ac.uk*

Compiled September 15, 2016

A programmable fiber long period grating (LPG) is experimentally demonstrated in a liquid core optical fiber with a low insertion loss. The LPG is dynamically formed by a temperature gradient in real-time through a micro-heater array. The transmission spectrum of the LPG can be completely reconfigured by digitally changing the grating period, index contrast, length and design. The phase-shift inside the LPG can also be readily defined to enable advanced spectrum shaping. Owing to the high thermo-optic coefficient of the liquid core, it is possible to achieve high coupling efficiencies with driving powers as low as a few tens of milliwatts. The proposed thermo-programmable device provides a potential design solution for dynamic all-fiber optics components. © 2016 Optical Society of America

OCIS codes: (050.2770) Gratings, (060.2310) Fiber optics; (060.2340) Fiber optics components

http://dx.doi.org/10.1364/ao.XX.XXXXXX

Reconfigurable optical devices that can respond dynamically to variable demands are required for the development of efficient and flexible all-fiber systems. Although silica fibers are an excellent platform for low loss waveguiding, they are somewhat limited in terms of their functionality owing to their low linear, nonlinear and thermal optical coefficients, for example. Therefore, in order to introduce some reconfigurable behavior into these fibers they are often infiltrated with materials that have tunable optical properties such as polymers [1], liquids [2], liquid crystals [3] and gases [4]. Of these hybrid-material structures liquid-filled optical fibers have been the most widely investigated owing to the relative ease of fabrication, but also because there is a long list of liquids that offer many useful properties for photonics applications including low loss, broadband transmission windows [5]. As a result, there have been a number of important device demonstrations in liquid-filled fibers in areas ranging from supercontinuum generation [6] to sensing [7, 8] and lasing [9].

A popular approach to introduce dynamic tunability into these hybrid fibers is to use a liquid with high thermo-optic coefficient (TOC) [10], so that the device properties can be altered with relatively minor temperature changes. Thus the energy requirements for temperature tuning are typically much lower than alternative methods, such as electro-optic modification where high driving voltages are usually required [11, 12]. However, as of to date, temperature tuning of the liquid-filled fibers has been limited to adjusting the operation wavelength and not the device function [2, 7, 8]. Clearly the ability to introduce localized temperature gradients along the length of the liquid core that would allow for reconfiguration of the device function would greatly expand the application potential of these fibers.

In this Letter, we present a new type of completely programmable liquid core optical fiber (LCOF) device where the optical functionality is imprinted onto the core using a micro-heater array (MHA). To demonstrate proof of concept, we use localized temperature-induced index changes to write a series of long period gratings (LPGs) into the LCOF. LPGs are of great interest for the development of in-fiber notch filters [13], optical fiber sensors [14] and spatial mode converters [15], and a variety of fabrication methods exist for their inscription into solid fibers such as UV radiation, stress, and/or structural-induced index changes [13, 16–19]. However, the reconfigurability of these permanently inscribed gratings is inherently quite limited. In contrast, here we demonstrate large, dynamic tuning of both the spectral profile and band rejection (BR) strength by digitally programming the individual heating elements in our MHA to control the grating period, strength, length and design. Owing to the high TOC of our liquid core, we show that it is possible to obtain a maximum BR higher than 20 dB in a range of different LPGs for driving powers as low as 55 mW.

To fabricate the LCOF device we made use of a mechanical splicing method described in [20]. Briefly, the LCOF is butt-coupled to the input and output single mode fibers (SMFs), with the connections held in place via a tapered capillary sleeves (inner waist diameters of around 127 μm). As well as helping to align the fiber cores, the sleeves also serve as reservoirs of excess liquid to ensure the core is always completely

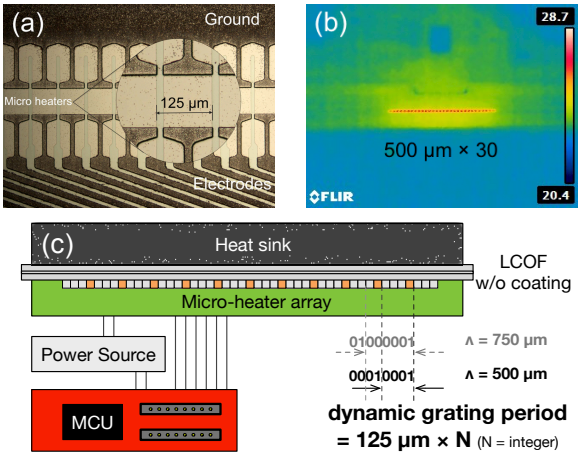

Fig. 1. (a) Microscopic image of the micro-heater array. (b) Thermal image of 30 activated micro-heaters, each separated by 500 μm. (c) Schematic showing the device design and grating period tuning mechanism. MCU: microcontroller unit.

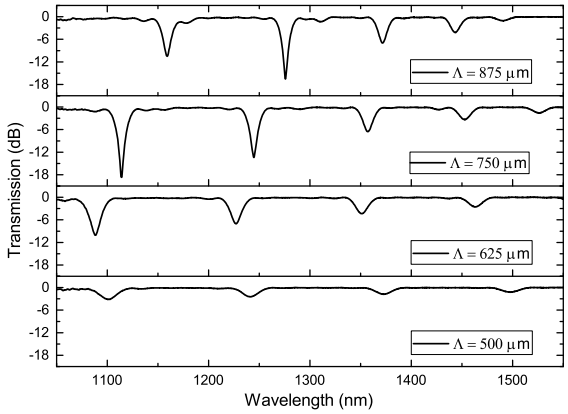

Fig. 2. Transmission spectra for reconfigured LCOF LPGs with different periods (as labeled in the legend).

filled. The ends of the sleeves are then sealed to ensure device stability and durability. The LCOF used in our work has a simple step index structure with dimensions similar to the SMFs (inner/outer diameters of 8.6 μm/125 μm) to facilitate coupling. For the liquid we use a mixture of carbon tetrachloride (CCl_4) and bromotrichloromethane ($BrCCl_3$) from *Sigma-Aldrich*, with a volume ratio of 15:1. The addition of a small amount of $BrCCl_3$ is required to raise the index slightly so that the modes are well confined to the core over the entire wavelength range of our investigations (1050 − 1550 nm), i.e., the LCOF is not weakly guiding [21]. We estimate the refractive index of the mixture to be $n_{mix} \sim 1.449$ at 1550 nm [5, 21], so that the LCOF only supports the fundamental mode with a mode area that is well matched to the SMFs. At this wavelength the total insertion loss of the 50 cm long LCOF is $\sim$ 0.5 dB, which, owing to the high transparency of the liquids, we attribute primarily to imperfections in the device fabrication associated with the fiber alignment and scattering at the joints [20]. We note that the length of the fibre was chosen for ease of handling and it could easily be reduced to a few centimeters depending on the application and packaging requirements.

The grating is written into the LCOF using the MHA shown in Fig. 1(a). The micro-heaters are connected in parallel, with a spacing of 125 μm, and each can be independently turned on or off via a microcontroller unit (MCU). The voltage applied to the MHA can also be controlled to tune the temperature, with a resolution of 0.01 V. Fig. 1(b) shows a thermal image of 30 activated micro-heaters, separated by 500 μm, while the applied voltage is set to 1.50 V to realize a strong visible contrast on the thermal camera. The MHA is then attached to the LCOF as shown in Fig. 1(c). To ensure a stable and uniform transfer of heat, the LCOF is stripped of its coating and aligned between the MHA and a heat sink. In the digital array that defines the grating profiles, '1' indicates an activated element, i.e., the micro-heater is on, while '0' represents off. Thus a grating that consists of sequences like "0001" defines a period of $\Lambda = 125\ \mu m \times 4 = 500$ μm, and the number of these periods N defines the grating length $L = N\Lambda$. By controlling the sequence of activated elements (period, length and position), and the applied voltage (i.e., the index contrast), the grating profile can be completely reconfigured and optimized in real-time. To restrict the experimental complexity, in this work all of the gratings will be written with only a single activated micro-heater in each period.

The simplest way to demonstrate tunability is to change the grating period and monitor the resonant wavelength λ_r shift, which is governed by the phase matching condition [13]:

$$\lambda_r = \delta n \cdot \Lambda, \tag{1}$$

where δn is the difference between the effective index of the core and cladding modes. This can be achieved by simply changing the separation between the activated heating elements, as illustrated via the coding schematic in Fig. 1(c). Fig. 2 shows the transmission spectra for the imprinted LPGs using an applied voltage of 0.50 V, with periods ranging from 500 μm to 875 μm and lengths of $L = 30\Lambda$. These spectra are measured $\sim$ 15 seconds after the programming to ensure stability, with the room temperature fixed at $\sim$ 23.0 °C, and have been normalized to remove the contributions of the coupling losses. Multiple transmission dips are observed associated with coupling to different cladding modes, with the resonant wavelengths shifting due to the changing pitch. Although the coupling can be quite strong for the gratings with $\Lambda > 600\ \mu$m, the BR reduces significantly for the shortest grating. We attribute this behaviour to the fact that when the spacing between the elements is small, the average core temperature increases, reducing the index contrast and ultimately placing a limit on the minimum grating period. We note that in period tuning the step size of 125 μm is only limited by the size of the individual heaters and could be reduced for finer tuning using state of the art micro-fabrication techniques.

Owing to the unique properties of the liquid core, we have used numerical modelling to better understand the behaviour of our LCOF LPG. Fig. 3 shows the calculated phase matching curves for different grating periods following the three-layer fiber model by Erdogan [22]. In our simulations we only consider cladding modes with azimuthal order of $l = 1$, and ν = odd integers (from 1 − 15), as these are the only modes that have a strong overlap with the core guided mode. The calculated curves are in excellent agreement with the experimentally determined resonant wavelengths from Fig. 2, where each symbol corresponds to a different grating period. Interestingly, these results show that the resonant wavelength decreases for increasing grating period, which is opposite to what happens in traditional LPG inscribed in SMFs [13]. This behaviour is due to the different dispersion properties of the liquid core compared

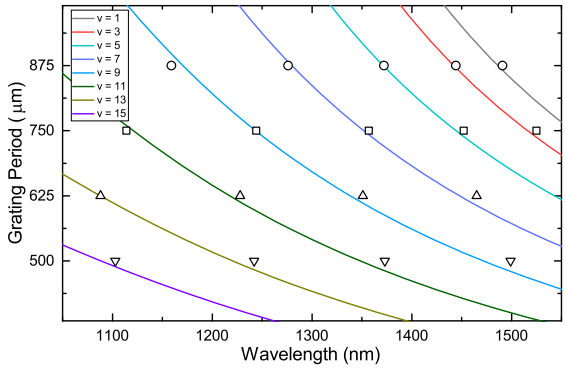

Fig. 3. Simulated phase matching curves showing the resonant wavelength shift for different grating periods in the LCOF LPG. Symbols mark the resonant wavelengths from Fig. 2. Each curve corresponds to coupling to a different cladding mode, $l = 1$ and ν as labeled in the legend.

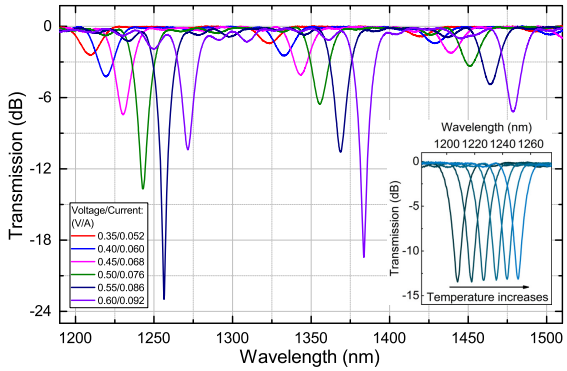

Fig. 4. Transmission spectra measured for different applied voltages and resulted current (as labeled in the legend). Inset shows total temperature tuning of 0.33 °C with equal steps.

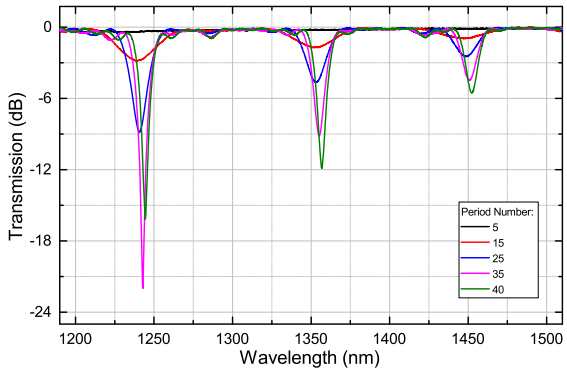

Fig. 5. Transmission spectra measured for different grating lengths ($L = N\Lambda$), where N is labeled in the legend.

to the silica cladding. In standard SMF the index difference between the core and cladding is fairly constant as a function of wavelength, but for our LCOF it increases for increasing wavelengths, which results in the negative slopes in Fig. 3. We can also see that, for a fixed grating period, coupling to higher order cladding modes occurs at shorter wavelengths, which explains why the transmission spectra show the trend of increasing coupling strength for decreasing wavelength, also opposite to traditional LPGs [22].

From the coupling efficiency (S) determined via Fig. 2, it is also possible to estimate the thermo-induced index change (Δn), and hence the associated temperature rise, via the relation [23]:

$$S = \sin^2\left(\frac{4\Delta n I L}{\lambda_r}\right). \tag{2}$$

Here I is the overlap integral between the core and cladding modes. Using the transmission spectrum corresponding to $\Lambda = 750\,\mu$m (duty cycle of 1/6), the index change is determined to be $\sim 1.5 \times 10^{-4}$. Thus, as the TOC of CCl_4 is -3.2×10^{-4} /°C [10], we can place an upper bound on the temperature rise of 2.75 °C for the applied voltage of 0.5 V. We note that this temperature change is considerably lower (by a factor of 50) than previous reports of thermo-induced LPG devices [24], which we attribute to the high TOC of the liquid and the high thermal conductivity of the silica cladding.

As seen in Eq. (2), the coupling efficiency is influenced by both the index contrast and the grating length. Thus a simple way to tune the efficiency is by adjusting the temperature of the MHA through the driving voltage. Fig. 4 shows the results of voltage tuning for a grating with $\Lambda = 750\,\mu$m and $L = 30\Lambda = 22.5$ mm. The results show the expected trend of a stronger and narrower rejection band as the index contrast increases, up until the point of over-coupling (as seen for the short resonant wavelength). The maximum BR of the grating is > 20 dB, while the out-of-band loss is as low as ~ 1 dB. Even at the highest voltage of 0.6 V, the power consumption of our device is only 55 mW, at least an order of magnitude lower than previous reports [24]. The increase in temperature associated with the higher driving voltage also causes the rejection bands to shift to longer wavelengths, a trend that can be explained by the material and waveguide properties: both the negative TOC of the liquid core and the negative slope of the phase matching curves result in a positive temperature response [25]. Further calculation for the cladding mode ($l = 1$, $\nu = 9$), with resonant wavelength around 1240 nm, shows a theoretical temperature sensitivity of $\sim$ 143.7 nm/°C, which fits well with the experimental result of $\sim$ 132.9 nm/°C (shown in the inset of Fig. 4). This provides further evidence of the advantages of a high-TOC material for thermally tuning of the device function [26]. Together with the voltage tuning, it offers an efficient method to tune the operation window of the LPG over a wide range. However, it is also possible to tune the efficiency via the grating length. To illustrate this Fig. 5 shows transmission spectra for a series of gratings with five different lengths, all taken for an applied voltage of 0.5 V and $\Lambda = 750\,\mu$m. Similar to the voltage tuning, the BR increases for increasing length up to the point of over-coupling. Again, the coupling efficiency is higher for the shorter resonant wavelengths, where the over-coupling happens first. This time, however, the resonant wavelength is much more stable as there is only a slight increase in the temperature associated with the increased number of heated elements. Consequently, it is possible to achieve high precision tuning simply by adjusting the voltage and/or the grating length by as little as a single period, and higher BR rate could be reached by optimizing both.

To further explore the advanced reconfigurability of the proposed device, in our final experiment a phase-shift is introduced into the center of the grating to reshape the rejection band. The grating parameters are set such that $\Lambda = 750\,\mu$m,

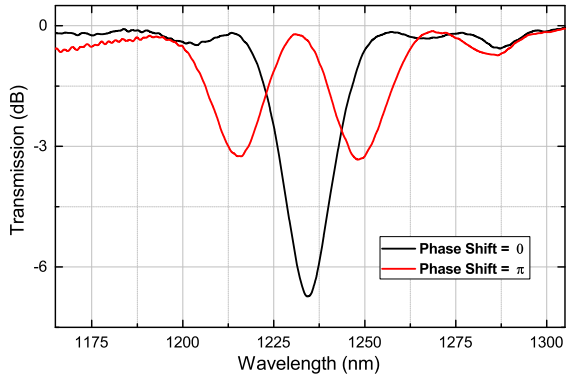

Fig. 6. Transmission spectra for a LPG with and without a π phase-shift in the center (as labeled).

$L = 24\Lambda = 18.00\,\text{mm}$ and the applied voltage is 0.5 V. Thus, the corresponding digital sequence for one grating period is "000001" and an added half period of "000" is positioned in between two full periods to act as the π phase-shift. Fig. 6 shows the transmission spectra of the gratings with and without the phase-shift. As expected, the π phase-shift opens up a transmission window at the wavelength of the original reject band, with two bands appearing symmetrically on either side. The almost equal-depth of the minima provides evidence of the homogeneous nature of the thermally induced grating and shows that phase-shifts can be easily introduced in a well-controlled manner via the digital encoded MHA.

As these thermally imprinted gratings feature low insertion and out-of-band losses, it will also be possible to cascade several gratings within a single LCOF. This would allow for unprecedented control of the spectral shaping, and thus the development of an array of devices such as filters, pulse shapers, etc [27]. The rate at which the gratings can be reconfigured will ultimately depend on the choice of materials and the device geometry. It is worth noting that for our particular case, as the thermal diffusivity of CCl_4 is an order of magnitude lower than silica ($\alpha_{CCl_4} = 8.24 \times 10^{-8}\,\text{m}^2/\text{s}$ vs $\alpha_{SiO_2} = 8.48 \times 10^{-7}\,\text{m}^2/\text{s}$), heat from the MHA is transferred rapidly through the cladding to the liquid core, where it can set up a stable temperature gradient. By tuning the CW laser to the resonant wavelength and monitoring the transmitted power, we determined the turn-on time to be $\sim$ 2.69 seconds, while the turn-off time was $\sim$ 0.04 seconds. However, as the turn-on time in this device is primarily limited by the thermal transfer through the thick silica cladding, a viable route to reducing this and the overall power consumption, would be to position the MHA closer to the core by reducing the cladding diameter or using a side-polished capillary for the liquid integration. Improving the encapsulation of the device would also result in more efficient and stable operation. Nevertheless, our device showed good durability and could be repeatedly programmed over continuous weeks.

In conclusion, a thermo-programmable LPG has been experimentally demonstrated in a LCOF device with low insertion loss. By digitally tuning the grating period, index contrast, length and design we have shown that it is possible to precisely control the position, strength and structure of the spectral rejection bands in real-time. Owing to the favourable properties of the liquid core, coupling efficiencies as high as 20 dB can be obtained for operation powers of only a few tens of milliwatts. As well as opening up new directions for reconfigurable fiber devices, this approach could also be applied to the rapidly developing field of optofluidics on-chip, where devices with increasingly complex functionality are being sought to shape and control the flow of light [28].

Funding. The China Scholarship Council (CSC) (201406230169); the Hong Kong Polytechnic University (Project G-SB17); the Engineering and Physical Sciences Research Council (EPSRC) (EP/J004863/1).

Acknowledgment. The authors thank Dr. Peter Shardlow and Timothy Hoad for the great technical assistance. The data for this Letter are accessible through the University of Southampton Institutional Research Repository (DOI: 10.5258/SOTON/400437).

REFERENCES

1. P. S. Westbrook, B. J. Eggleton, R. S. Windeler, A. Hale, T. A. Strasser, and G. L. Burdge, IEEE Photon. Technol. Lett. **12**, 495 (2000).
2. P. Steinvurzel, E. D. Moore, E. C. Mägi, and B. J. Eggleton, Opt. Lett. **31**, 2103 (2006).
3. T. T. Larsen, A. Bjarklev, D. S. Hermann, and J. Broeng, Opt. Express **11**, 2589 (2003).
4. N. Y. Joly, J. Nold, W. Chang, P. Hölzer, A. Nazarkin, G. K. L. Wong, F. Biancalana, and P. S. J. Russell, Phys. Rev. Lett. **106**, 203901 (2011).
5. S. Kedenburg, M. Vieweg, T. Gissibl, and H. Giessen, Opt. Mater. Express **2**, 1588 (2012).
6. D. Churin, T. N. Nguyen, K. Kieu, R. A. Norwood, and N. Peyghambarian, Opt. Mater. Express **3**, 1358 (2013).
7. L. Rindorf and O. Bang, Opt. Lett. **33**, 563 (2008).
8. Y. Yu, X. Li, X. Hong, Y. Deng, K. Song, Y. Geng, H. Wei, and W. Tong, Opt. Express **18**, 15383 (2010).
9. R. M. Gerosa, A. Sudirman, L. de S. Menezes, W. Margulis, and C. J. S. de Matos, Optica **2**, 186 (2015).
10. K. Moutzouris, M. Papamichael, S. C. Betsis, I. Stavrakas, G. Hloupis, and D. Triantis, Applied Physics B **116**, 617 (2014).
11. L. Wei, J. Weirich, T. T. Alkeskjold, and A. Bjarklev, Opt. Lett. **34**, 3818 (2009).
12. D. Zhang, J. Kang, W. Wong, D. Yu, and E. Y. Pun, Opt. Lett. **40**, 4715 (2015).
13. A. M. Vengsarkar, P. J. Lemaire, J. B. Judkins, V. Bhatia, T. Erdogan, and J. E. Sipe, J. Lightwave Technol. **14**, 58 (1996).
14. S. W. James and R. P. Tatam, Meas. Sci. Technol. **14**, R49 (2003).
15. D. J. Richardson, J. M. Fini, and L. E. Nelson, Nat. Photonics **7**, 354 (2013).
16. I. K. Hwang, S. H. Yun, and B. Y. Kim, Opt. Lett. **24**, 1263 (1999).
17. J. H. Lim, K. S. Lee, J. C. Kim, and B. H. Lee, Opt. Lett. **29**, 331 (2004).
18. Y. N. Zhu, P. Shum, H. W. Bay, M. Yan, X. Yu, J. J. Hu, J. Z. Hao, and C. Lu, Opt. Lett. **30**, 367 (2005).
19. Y. Wang, W. Jin, J. Ju, H. Xuan, H. L. Ho, L. Xiao, and D. Wang, Opt. Express **16**, 2784 (2008).
20. L. Xiao, N. V. Wheeler, N. Healy, and A. C. Peacock, Opt. Express **21**, 28751 (2013).
21. A. R. Chraplyvy and T. J. Bridges, Opt. Lett. **6**, 632 (1981).
22. T. Erdogan, J. Opt. Soc. Am. A **14**, 1 (1997).
23. E. M. Dianov, D. S. Stardubov, S. A. Vasiliev, A. A. Frolov, and O. I. Medvedkov, Opt. Lett. **22**, 1 (1997).
24. M.-S. Kwon and S.-Y. Shin, IEEE Photon. Technol. Lett. **17**, 145 (2005).
25. X. W. Shu, L. Zhang, and I. Bennion, J. Lightwave Technol. **20**, 255 (2002).
26. K. S. Chiang, K. P. Lor, C. K. Chow, H. P. Chan, V. Rastogi, and Y. M. Chu, IEEE Photon. Technol. Lett. **15**, 1094 (2003).
27. M. Kulishov and J. Azana, Opt. Lett. **30**, 2700 (2005).
28. H. Schmidt, A. R. Hawkins, and L. E. Nelson, Nat. Photonics **5**, 598 (2011).